

Elementary transitions and magnetic correlations in two-dimensional disordered nanoparticle ensembles

G. M. Pastor

*Institut für Theoretische Physik, Universität Kassel,
Heinrich Plett Straße 40, 34132 Kassel, Germany*

P. J. Jensen

*Institut für Theoretische Physik, Freie Universität Berlin,
Arnimallee 14, 14195 Berlin, Germany*

Abstract

The magnetic relaxation processes in disordered two-dimensional ensembles of dipole-coupled magnetic nanoparticles are theoretically investigated by performing numerical simulations. The energy landscape of the system is explored by determining saddle points, adjacent local minima, energy barriers, and the associated minimum energy paths (MEPs) as functions of the structural disorder and particle density. The changes in the magnetic order of the nanostructure along the MEPs connecting adjacent minima are analyzed from a local perspective. In particular, we determine the extension of the correlated region where the directions of the particle magnetic moments vary significantly. It is shown that with increasing degree of disorder the magnetic correlation range decreases, i.e., the elementary relaxation processes become more localized. The distribution of the energy barriers, and their relation to the changes in the magnetic configurations are quantified. Finally, some implications for the long-time magnetic relaxation dynamics of nanostructures are discussed.

PACS numbers: 75.75.+a, 75.60.Jk, 75.50.Lk,

I. INTRODUCTION

Two-dimensional (2D) ensembles of interacting magnetic nanoparticles are currently the subject of an intense fundamental and technological research activity.^{1,2} The magnetic particles in these systems are subject to both local couplings and long-range interactions. By varying the interparticle distance the relative importance of these two contributions can be tuned to a certain extent. The magnetic response can then be correlated with the size distribution and the geometrical arrangement of the nanoparticles, the latter being experimentally accessible through a number of microscopy techniques. Of particular interest is the slow magnetic dynamics,³ like magnetic ageing, rejuvenation, or magnetic viscosity.⁴ These non-equilibrium effects are reminiscent of the spin glass behavior observed in impurity spin systems with nonuniform exchange couplings.⁵ In fact, the magnetic nanostructures studied in this paper can be viewed as a super-spin glass with giant magnetic moments that interact via the dipole coupling.

One of the experimental approaches to 2D nanostructures derives from investigations of three-dimensional (3D) ferrofluids consisting of non-overlapping magnetic particles in a liquid or frozen solvent.⁶ The controlled preparation of 2D nanoparticle ensembles with different degrees of structural and magnetic disorder has recently become feasible by reducing the thickness of 3D ferrofluids to within a few particle diameters.^{1,7,8} A second experimental approach to 2D magnetic nanosystems stems from the study of thin magnetic films that are grown by depositing atoms on nonmagnetic substrates.^{9,10,11,12} In the early stages of film growth, before a continuous layer is formed, it is possible to obtain a controlled distribution of magnetic islands that interact by long-range forces like dipole coupling or Ruderman-Kittel-Kasuya-Yosida (RKKY) interactions in case of metallic substrates.¹³ As a consequence of the preparation conditions, these magnetic nanostructures are usually characterized by the presence of a considerable degree of structural disorder. This manifests itself, for instance, in the particle-size dispersion or in the irregularity of the particle arrangement.

The magnetic behavior of magnetic nanostructures is determined by the interplay between single-particle properties (e.g., magneto-crystalline or shape anisotropies) and interparticle effects (e.g., dipolar, RKKY or exchange interactions). For weakly cou-

pled systems the local contributions dominate, and the interactions can be handled as perturbations. In this case the magnetic relaxation is governed by single-particle fluctuations that can be described by a superparamagnetic Arrhenius-like model showing blocking effects at low temperatures.¹⁴ However, in the most interesting case of strongly interacting magnetic nanostructures, for example, for densely packed nanoparticles, the single-particle approach is no longer appropriate.² Here the system exhibits a complicated, spin-glass-like behavior, characterized by a complex energy landscape, a large number of metastable minima, and a non-collinear magnetization of the particle ensemble.^{15,16} For these strongly interacting systems the magnetization dynamics is determined by a collective response. In other words, changes in the magnetization direction of a given particle inevitably cause neighboring particles to vary their magnetic directions as well. During the transition from a local energy-minimum to another one, within a magnetic relaxation process, the magnetization directions of many particles change. Therefore, the collective behavior of the nanostructure has to be taken into account from the start.

The disorder within the nanostructure and the anisotropic long-ranged nature of the dipole interaction represent a serious challenge for theoretical investigations so that simple analytical approaches are in general not applicable. Therefore, numerical simulations have been performed in order to achieve a detailed description of these systems.¹⁷ Phenomenological, macroscopic quantities like the field-cooled and zero-field-cooled magnetization curves, the linear and nonlinear susceptibilities, or the magnetic relaxation rate have been calculated.^{8,18,19,20} Moreover, the magnetic transitions between energy minima have been investigated by solving a continuum dynamical model including dissipation and thermal fluctuation terms (Langevin dynamics) as well as by using path-integral methods.²¹ In order to take into account the diversity of nonequivalent trajectories, these calculations involve optimizations in a space of dimension $d = n\nu k$, where n is the number of particles, ν the number of degrees of freedom, and k the number discretizations of the relaxation path.

The main purpose of this paper is to investigate the collective microscopic processes occurring along the magnetic relaxations of disordered magnetic nanostructures. To this aim we focus on the elementary transitions along the minimum energy path (MEP) connecting two neighboring local minima across a single saddle point. These fundamental

processes can be regarded as the microscopic analogy to the Barkhausen-jumps of the magnetization in hysteresis loops. The actual macroscopic relaxation is the result of a succession of such transitions between metastable states. Understanding them is therefore very important for the modelization of the long-time dynamics. One of the goals of this work is to analyze the properties of these magnetic rearrangements from a local perspective by determining the variations $\Delta\phi_i$ in the directions of the magnetic moments at each nanoparticle i . In particular a correlation range λ_c is defined, that measures the spatial extent of the relevant collective processes as a function of experimentally important parameters like particle density and degree of disorder. Furthermore, the distribution of the energy barriers is quantified in order to determine how they correlate with the changes in the magnetic configurations.

The remainder of the paper is organized as follows. In Sec. II the theoretical background describing the interacting magnetic nanoparticle system is presented. The methods for calculating saddle points, adjacent minima, relaxation paths and the resulting changes in the magnetic order along elementary transitions are outlined. In Sec. III representative results for the elementary transitions and the associated correlation ranges are reported and discussed. The distribution of the energy barriers, and their relation to the variation in the magnetic configurations are investigated. Finally, we conclude in Sec. IV by pointing out some of the potential implications of this study for magnetization reversal dynamics and high-density magnetic recording.

II. MODEL AND CALCULATION METHOD

The purpose of this section is to describe the main aspects of the present model of disordered magnetic nanostructures. Further details of the theory may be found in Ref. 16. We consider a 2D system of N non-overlapping, spherical magnetic particles contained in a square unit cell with periodic boundary conditions. Due to the strong interatomic ferromagnetic exchange interactions and the small size of the particles under consideration, it is clear that each particle i can be regarded as a single-domain or Stoner-Wohlfarth magnet carrying a giant spin \mathbf{m}_i .²² The modulus of the local moments is given by $m_i = n_i \mu_{at}$, where μ_{at} is the atomic magnetic moment and n_i the number of atoms in particle i .

Different kinds of structural arrangements are considered in the following: (i) a periodic square-lattice array, (ii) a disordered array where the particles are randomly dispersed around the sites of a periodic square lattice according to a Gaussian distribution with standard deviation σ_R , and (iii) a fully-random particle distribution of non-overlapping particles within the unit cell.

In this paper we focus on the effects of the dipole coupling on the collective magnetic behavior. This is a particularly interesting physical situation, since in the limit of weak magnetic anisotropy and external magnetic field the numbers of local minima and the complexity of the energy landscape are expected to be largest. For each particle arrangement the dipolar interaction between the particle moments \mathbf{m}_i is given by

$$E = \frac{\mu_0}{2} \sum_{i \neq j} [\mathbf{m}_i \cdot \mathbf{m}_j r_{ij}^{-3} - 3 (\mathbf{r}_{ij} \cdot \mathbf{m}_i) (\mathbf{r}_{ij} \cdot \mathbf{m}_j) r_{ij}^{-5}] , \quad (1)$$

where $\mathbf{r}_{ij} = \mathbf{r}_i - \mathbf{r}_j$ is the vector between the centers of particles i and j , $r_{ij} = |\mathbf{r}_{ij}|$ the corresponding distance, and μ_0 the vacuum permeability. The infinite range of the dipole interaction is taken into account by computing an Ewald-type summation over all periodically arranged unit cells of the extended planar system.²³ Since the particles do not have direct metal-metal contacts, no interparticle exchange interactions are included. Taking into account these short-range contributions, as well as local magnetic anisotropies or external magnetic fields, poses no major technical difficulties and could be investigated by similar simulations. For simplicity we assume that all particles have the same size $n_i = 30000$ atoms, which corresponds to a particle radius of about 15 lattice constants. Previous studies have actually shown that the dominant disorder effects are due to the irregularity of the particle arrangement and that the distribution of particle sizes yields a similar behavior.¹⁶ The directions of the particle magnetizations \mathbf{m}_i are restricted to the plane of the nanostructure. Hence, the magnetic configurations are characterized for simplicity by the set of in-plane angles $\{\phi_i\}$ in the unit cell ($i = 1, \dots, N$).

The particle ensemble is characterized by the number of particles N in the unit cell, by the standard deviation σ_R of the structural disorder of the particle array, and by the surface coverage C .¹⁶ The size of the unit cell is defined in terms of N and the average interparticle distance R_0 . For a given realization of the nanostructure we sample randomly the energy landscape and determine a large number of first-order saddle points

(SPs) or transition states. These are characterized by having one negative eigenvalue of the Hessian of the interaction energy E [see Eq. (1)]. To locate the SPs we use a variant of the eigenvector-following method that is based on the eigenvalues and eigenvectors of the Hessian matrix as described in the Appendix. The two neighboring energy minima adjacent to each SP and the associated MEP are obtained by a simple steepest descent procedure starting at the SP along the negative-curvature direction. In this way the elementary relaxation path, the energies E_S and $E_{M_{1,2}}$ for the saddle point S and adjacent minima M_1 and M_2 , as well as the corresponding sets of magnetization angles $\{\phi_i(S)\}$ and $\{\phi_i(M_{1,2})\}$, are determined. In this context it is interesting to mention that loop-like paths also exist, where the SP connects a local minimum with itself via a closed loop (i.e., $M_1 = M_2$). The presence of these features of the energy landscape is favored by the periodicity of the angular functions entering Eq. (1). Nevertheless, loop-like MEPs have been excluded from the present analysis, since they do not contribute to the magnetic relaxation.

The range λ_c of the magnetic correlations involved in an elementary transition is quantified in two steps as follows. First, the epicenter \mathbf{R}_c of the angular variations $\Delta\phi_i = |\phi_i(M_1) - \phi_i(M_2)|$ between the two adjacent minima is determined from

$$\mathbf{R}_c = \frac{\sum_i \Delta\phi_i \mathbf{r}_i}{\sum_i \Delta\phi_i}, \quad (2)$$

where \mathbf{r}_i is the position of the center of particle i . Note that \mathbf{R}_c needs not to coincide with the position of any particle. Second, the dependence of $\Delta\phi_i$ on the distance $|\mathbf{r}_i - \mathbf{R}_c|$ to the epicenter is fitted by an exponential of the form

$$\Delta\phi_i = \Delta\phi_{\max} \exp(-2|\mathbf{r}_i - \mathbf{R}_c|/\lambda_c), \quad (3)$$

from which the correlation range λ_c is obtained. The angular variations are normalized with respect to the maximal change $\Delta\phi_{\max}$ occurring in that particular pair of states. The factor 2 in the exponential is introduced in order that λ_c covers most of the significant angular variations. Hence, for $|\mathbf{r}_i - \mathbf{R}_c| = \lambda_c$ the change of angle $\Delta\phi_i$ is reduced by a factor e^2 with respect to $\Delta\phi_{\max}$. However, the use of an exponential fit should not be interpreted as a statement on the precise distance dependence of $\Delta\phi_i$, which is presently not known in detail.

The Euclidean distance between the saddle point S and the adjacent minimum M is given by

$$D_{\text{SM}} = \{1 - \frac{1}{N} \sum_{i=1}^N \cos [\phi_i(S) - \phi_i(M)]\}^{1/2}. \quad (4)$$

D_{SM} provides a quantitative measure of the changes in the magnetic order during an elementary transition. The correlation ranges λ_c and distances D_{SM} are averaged over a large number of elementary transitions (typically a few thousands) and several geometrical arrangements of the particles in the nanostructure. In the following calculations parameters appropriate for Fe particles are used, i.e., $\mu_{at} = 2.2 \mu_B$ and nearest neighbor distance $a_0 = 2.5 \text{ \AA}$.

III. RESULTS AND DISCUSSION

The most stable magnetic arrangement of a periodic square lattice of dipole coupled magnetic nanoparticles having all the same size is known to correspond to the so-called microvortex state.¹⁶ This magnetic order has a vanishing net magnetization and is characterized by a continuous degeneracy with respect to the microvortex angle. Any, however small, deviation from the square-lattice symmetry lifts this degeneracy. For weak disorder the low-energy states preserve a close resemblance with a microvortex state but as the disorder increases the apparent extended periodicity of the magnetic structure is completely lost. In the case of strong disorder the magnetic state is characterized by head-to-tail arrangements of the particle moments and by local flux closures of the magnetization profile. In this Section results are presented and discussed for the correlation range λ_c , the energy barriers $\Delta E_{\text{SM}} = E_S - E_M$, and the distances D_{SM} , including averages over many elementary transitions as well as different values of the parameters N , σ_R and C characterizing the magnetic nanostructure.

Figure 1 illustrates typical examples of elementary magnetic transitions. The arrows refer to the magnetic directions of two adjacent minima, and the different shadings indicate the importance of the associated angular changes $\Delta\phi_i$. Two different structural arrangements are considered: a) an almost periodic square-lattice array with $\sigma_R = 5\%$, and b) a fully-random particle setup. The resulting correlation range λ_c is indicated by a

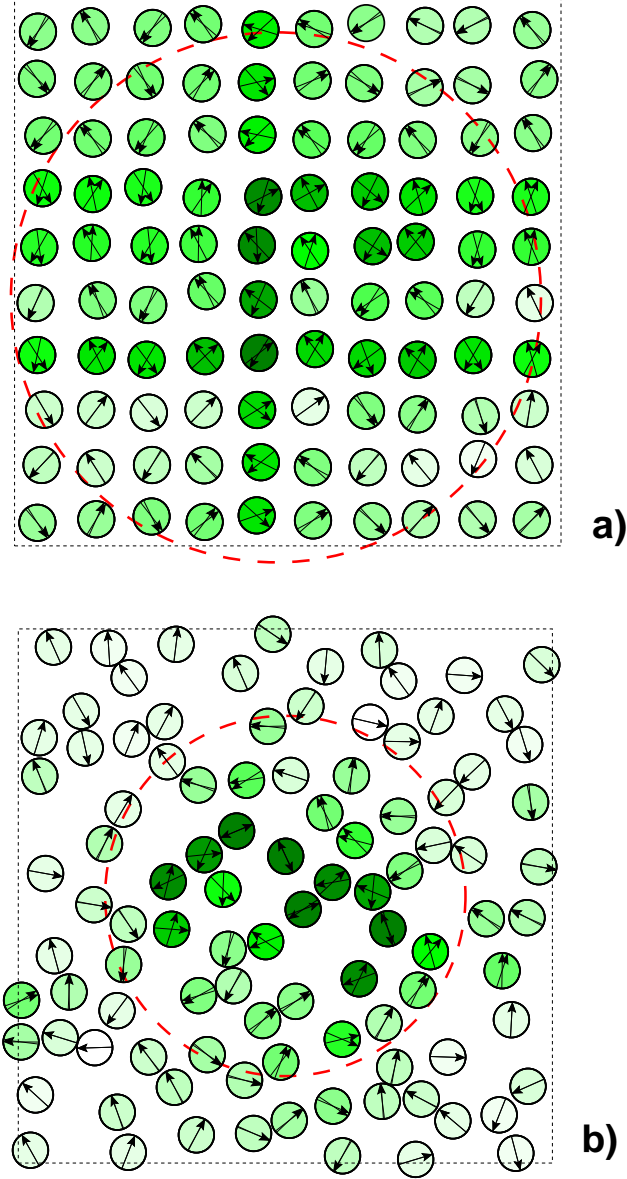


FIG. 1: (Color online) Illustration of elementary transitions in dipole-coupled nanostructures having a) a weak disorder with $\sigma_R = 5\%$, and b) a random particle distribution. In both cases the unit cell (dotted frame) contains $N = 100$ particles and the coverage is $C = 0.35$. The arrows show the directions of the magnetic moments corresponding to two adjacent local minima that are separated by a single energy barrier. The shading indicates the importance of the changes in the direction of the local moments. The dashed circle refers to the correlation range λ_c where the angular variations are most significant.

dashed circle. One clearly observes that λ_c is significantly larger for the almost periodic arrangement than for the random ensemble. In fact, in the former case λ_c is often comparable with the size of the unit cell. Hence, to obtain reliable quantitative results one would have to consider a much larger cell so that spurious effects from the periodic boundary conditions are avoided. In contrast, for strong disorder the region with significant orientational changes of \mathbf{m}_i remains quite small. In this case the results for λ_c are not affected by considering even larger unit cells. The magnetic transition presented in Figure 1(b) refers to a relatively large λ_c , usually the regions of significant magnetic variations for this kind of arrangement are somewhat smaller. Note that for small disorder, Figure 1(a), the magnetic variations are not isotropic but still reflect the square symmetry.

In order to derive a quantitative estimate of λ_c we approximate the dependence of $\Delta\phi_i$ on $|\mathbf{r}_i - \mathbf{R}_c|$ by an exponential law [see Eq. (3)]. Figure 2 shows the correlation range $\bar{\lambda}_c$ averaged over a large number of elementary transitions as a function of the structural disorder σ_R . A single realization of the nanostructure is considered either for different coverages C keeping the number N of particles in the unit cell constant, or vice versa. Results are given for $\bar{\lambda}_c$ and for the standard deviation $\Delta\lambda_c = \sqrt{\langle(\lambda_c - \bar{\lambda}_c)^2\rangle}$ in units of the average interparticle distance R_0 . Notice that R_0 increases as the coverage C is reduced. One observes that both $\bar{\lambda}_c$ and $\Delta\lambda_c$ decrease rapidly with increasing σ_R . Already for $\sigma_R > 10\text{--}20\%$ their values are practically indistinguishable from those of a random particle ensemble. Usually $\bar{\lambda}_c/R_0$ does not depend strongly on the coverage C , except for the largest values (e.g., $C = 0.55$) where the non-overlap constraint and the assumed small size dispersion force the particles to adopt an almost periodic arrangement. All the calculations for different numbers N of particles in the unit cell yield very similar results within the statistical uncertainty. In particular the elementary transitions illustrated in Fig. 1 correspond to relatively large correlation ranges. Moreover, notice that for small structural disorder $\sigma_R \leq 5\%$ and for small N our results for $\bar{\lambda}_c$ might not be very accurate quantitatively, since in these cases the correlation range is comparable to the size of the unit cell.

The regions where the elementary transitions take place become more localized with increasing disorder of the nanostructure. Beyond λ_c , in the remaining part of the unit cell, no significant changes in the directions of the particle magnetizations are found. The

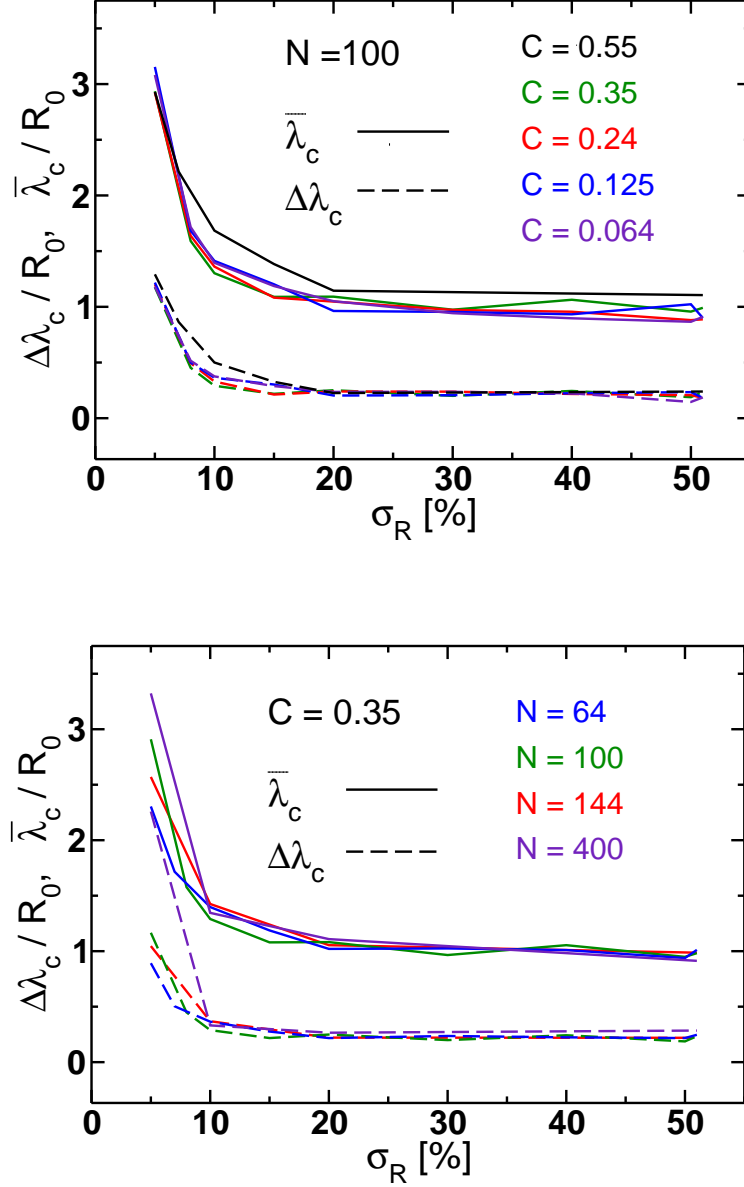


FIG. 2: (Color online) Average correlation range $\bar{\lambda}_c$ and standard deviation $\Delta\lambda_c$ as functions of the structural disorder σ_R . The results are obtained by sampling a large number of elementary transitions. In the top figure different coverages C are considered, while in the bottom figure the number of particles N in the unit cell is varied.

magnetic transitions in strongly interacting particle ensembles can be studied by using periodic cells provided that they are significantly larger than λ_c . For strong disorder already small unit cells suffice, whereas for almost periodic ensembles much larger cells are required. This renders the simulations far more demanding since an important number

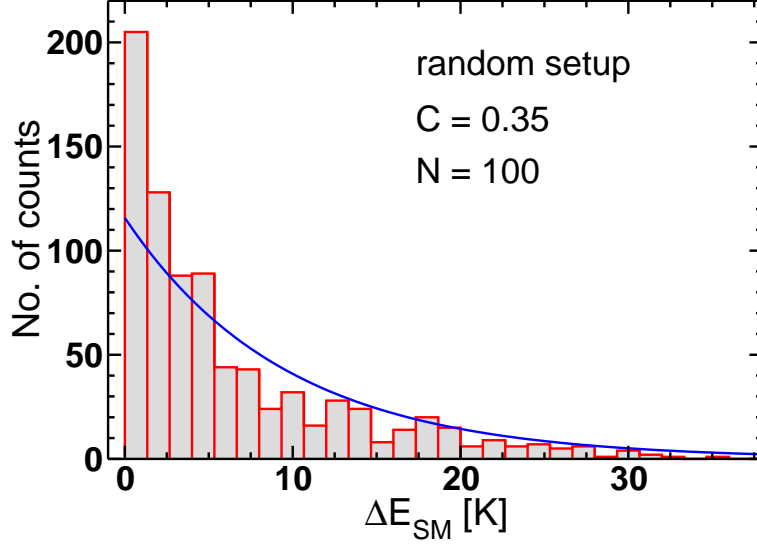


FIG. 3: (Color online) Distribution of the energy barriers ΔE_{SM} corresponding to the elementary transitions in a random ensemble having a coverage $C = 0.35$. The curve shows a fitted exponential law.

of particles takes part in an elementary transition. In the limit of a periodic arrangement the whole system is involved in an elementary relaxation (microvortex state). Nevertheless, for moderately disturbed ensembles where the underlying square arrangement is still clearly recognizable, the correlation range already assumes relatively small values [see, for example, Fig. 1(a)]. It would be therefore interesting to investigate the dependence of λ_c on σ_R in more detail, particularly as the periodic lattice is approached ($\sigma_R \rightarrow 0$). Finally, it should be mentioned that including single-particle magnetic anisotropies in the calculations would tend to further reduce λ_c , especially for small coverages C and large interparticle distances R_0 . This corresponds to weakly interacting particle ensembles, where the elementary transitions are essentially given by the magnetic reversal of a single particle.

The energy barriers $\Delta E_{\text{SM}} = E_S - E_M$ between a saddle point and the adjacent minima are one of the central properties governing the relaxation dynamics. In Fig. 3 the distribution of ΔE_{SM} is shown for a random ensemble having a coverage $C = 0.35$. The results were derived taking into account 826 different elementary transitions of the same nanostructure. One observes that the probability density of finding an energy barrier ΔE_{SM}

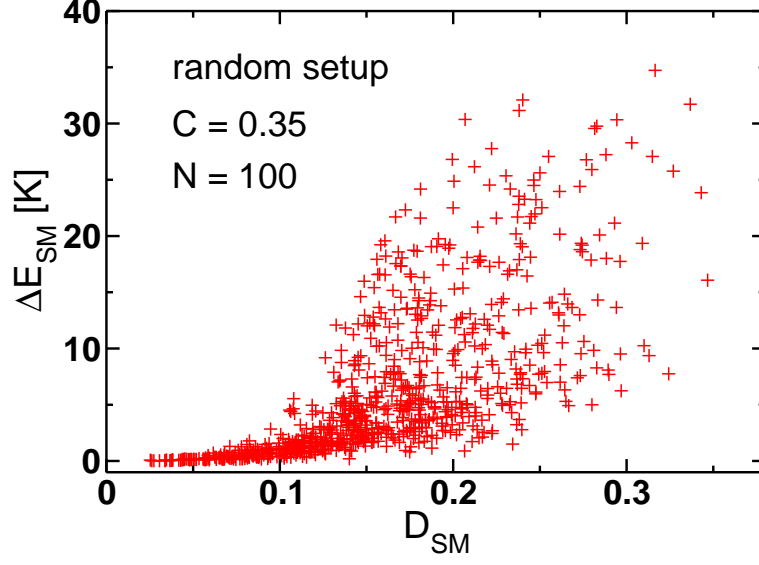


FIG. 4: (Color online) Scatter plot of the energy barrier ΔE_{SM} as a function of the distance D_{SM} between a saddle point and the adjacent local minima. As in Fig. 3 the particle setup is random and the coverage is $C = 0.35$.

follows approximately an exponential behavior, although the precise energy dependence of the distribution is not known. In any case, it is worth noting that the distribution of barrier energies contrasts with those of the absolute energies of the saddle points and local minima, which were shown to be Gaussian-like for random particle ensembles.¹⁶

Figure 4 shows the correlation between ΔE_{SM} and the distance D_{SM} between the saddle points and the adjacent minima in a random nanoparticle setup [see Eq.(4)]. As a general trend one observes that if D_{SM} is small also the corresponding ΔE_{SM} is small. However, for larger D_{SM} the energy barriers can assume both large and small values. Hence, important changes of the magnetic arrangement are also possible by involving only a single and relatively small energy barrier ΔE_{SM} . In this connection it should be noted that the distribution of the distances D_{SM} between saddles and minima has been found to follow a Poisson-like distribution.¹⁶

In Fig. 5 the average distance \overline{D}_{SM} and the standard deviation $\Delta D_{\text{SM}} = \sqrt{\langle (D_{\text{SM}} - \overline{D}_{\text{SM}})^2 \rangle}$ are given as functions of the structural disorder σ_R for different coverages C . \overline{D}_{SM} provides a measure of the change in the magnetic state associated with an elementary transition. In agreement with the results for λ_c shown in Fig. 2, \overline{D}_{SM} decreases

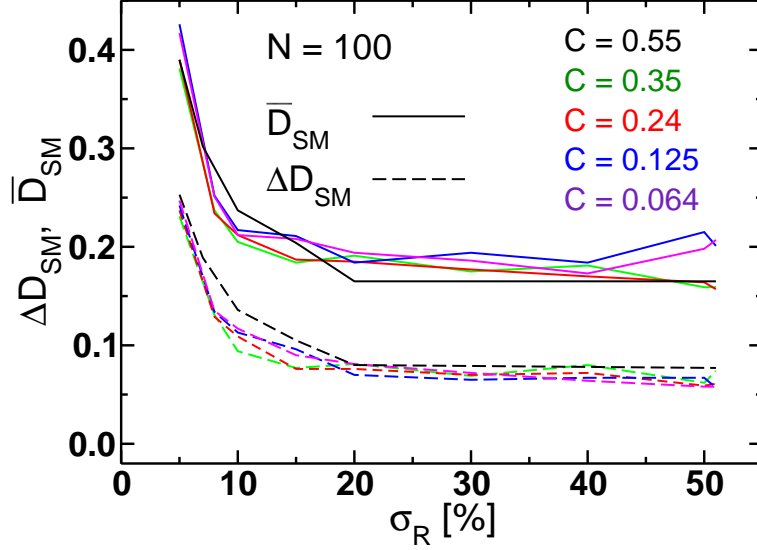


FIG. 5: (Color online) Average distance \bar{D}_{SM} between saddle points and adjacent minima, as well as the standard deviation $\Delta D_{SM} = \sqrt{\langle (D_{SM} - \bar{D}_{SM})^2 \rangle}$ as functions of the structural disorder σ_R . The results are derived from a large number of elementary transitions for each different coverage C .

with increasing σ_R , converging to the random-setup limit already for $\sigma_R \geq 20\%$. No significant dependence on the coverage C is found. The distance between the neighboring minima of elementary transitions (D_{MM}) follows closely the behavior of D_{SM} , of course with somewhat larger values. As in the case of Fig. 2 the results for weak structural disorder $\sigma_R \leq 5\%$ are less reliable due to the finite size of the periodic cell.

IV. CONCLUSION

The elementary relaxation processes occurring in disordered 2D ensembles of dipole-coupled magnetic nanoparticles have been investigated by calculating the transitions between neighboring metastable states across first-order saddle points. For this purpose an eigenvector-following method was implemented. The extension of the correlated region where the magnetic directions of the particles vary significantly has been calculated. In particular we have shown that the magnetic correlation range λ_c becomes smaller as the degree of disorder in the nanostructure increases. The tendency to localization of elemen-

tary transitions in disordered magnetic systems renders the simulation of these structures computationally less demanding. Moreover, the distribution of the energy barriers ΔE_{SM} has been found to follow approximately an exponential behavior. An analysis of the relation between ΔE_{SM} and the change D_{SM} of the magnetic state shows that small energy barriers can lead to both small and large magnetic relaxations, whereas large barriers always imply an important rearrangement of the magnetic state.

A number of implications and open questions related to our results may be pointed out. As already noted, the time evolution of the magnetization of the nanostructure can be described by a succession of the elementary transitions investigated in this work. Particularly important for the description of such processes is the knowledge of the connectivity of the network of metastable states in the complex spin-glass-like energy landscape. For each given system one would have to determine which minima are connected by elementary transitions, as well as the corresponding transition rates. The latter are mainly defined by the energy barrier, the eigenfrequencies at the saddle point, and the length of the MEP. They can be determined in the framework of transition-state theory including finite-temperature effects. Besides the elementary transitions involving collective rotations of the particles moments within a limited correlation range, the magnetic relaxation of the nanostructure as a whole involves some complex domain-wall-like motion that results from a sequence of elementary processes. In the case of time-dependent fields, averages over trajectories should be performed in order to simulate hysteresis loops from a microscopic point of view.

For more realistic simulations and for a detailed comparison with experiment it would be interesting to take into account other potentially important contributions, for example, the magnetic anisotropy energy of individual particles and the interaction with external magnetic fields. Qualitatively, one expects that increasing the single-particle anisotropies or the applied field should tend to reduce the correlation range of the elementary dynamical process, since the magnetic relaxation would be increasingly dominated by single-particle effects. Another aspect deserving further study concerns the distribution of particle sizes, which is certainly unavoidable in real nanostructures. In fact previous works²⁴ suggest that they should have similar, probably less severe consequences on the energy landscape as the positional disorder considered here. More interesting interaction

effects on the dynamics are expected to result from other types of interparticle couplings, for instance, indirect RKKY interactions between NP on metallic substrates, or direct exchange interactions at the boundaries of bare NPs in contact. These energy contributions can be treated straightforwardly using the methods developed in this work.

The trend to increasing localization of the magnetic excitations with increasing disorder in the particle arrangement should be of interest for tailoring materials for information storage. In fact, a stronger disorder decreases the minimum distance required for an independent switching of neighboring ‘bits’. Hence, controlling the main parameters characterizing the nanostructure allows to optimize their magnetic response as potential high-density magnetic-storage media or spintronic devices, for example, by tuning the particle arrangements and the coverages. This also reveals the limits for single-particle read and write processes in interacting magnetic nanostructures. Research in these directions is currently in progress.

APPENDIX A: ITERATIVE SEARCH FOR SADDLE POINTS

The method to determine the first-order saddle points is based on the eigenvalues and eigenvectors of the Hessian matrix of the energy E as a function of the magnetization angles $\{\phi_i\}$ [see Eq. (1)].²⁵ The following iteration algorithm is applied as sketched in Fig. 6: (i) Consider an arbitrary initial magnetic state $\mathbf{P}^{(k)}$ in the N -dimensional space of the magnetization angles $\{\phi_i\}$. (ii) Determine at $\mathbf{P}^{(k)}$ the eigenvector $\mathbf{v}_0^{(k)}$ of the Hessian corresponding to the lowest eigenvalue $\lambda_0^{(k)}$. (iii) Maximize the energy of the magnetic state \mathbf{P} along $\mathbf{v}_0^{(k)}$ until a state \mathbf{P}_0 is found where the energy shows a maximum along $\mathbf{v}_0^{(k)}$, or until a maximal prescribed distance from $\mathbf{P}^{(k)}$ is reached. (iv) Starting now from \mathbf{P}_0 minimize the energy in the $(N - 1)$ -dimensional space perpendicular to $\mathbf{v}_0^{(k)}$ until the nearest minimum in this restricted subspace is reached. (v) Set this minimum as the initial state $\mathbf{P}^{(k+1)}$ of the next iteration step, and repeat steps (ii)–(iv) until a saddle point \mathbf{S} is reached with the desired accuracy. This procedure is similar to the eigenvector-following method described in Ref. 26.

The convergence criterion at a first-order saddle point \mathbf{S} requires that the norm of the gradient be sufficiently small, that the lowest eigenvalue λ_0 at \mathbf{S} be negative, and that

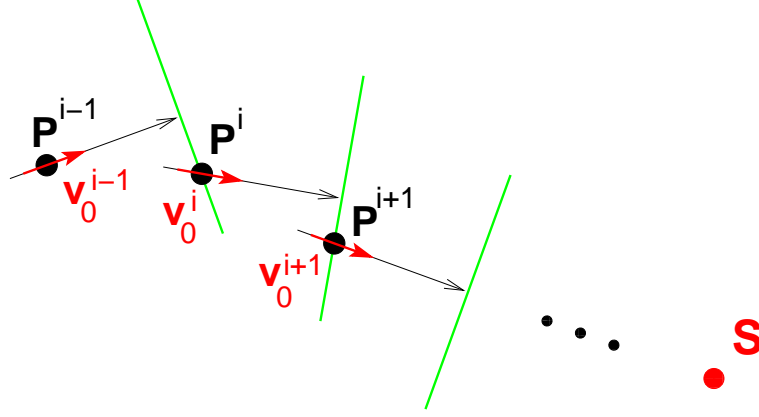


FIG. 6: (Color online) Sketch of the eigenvector-following method to determine first-order saddle points.

all other eigenvalues be positive. The two corresponding minima M_1 and M_2 adjacent to a saddle point are then determined by descending from the saddle point along the two opposite directions defined by the eigenvector \mathbf{v}_0 corresponding to λ_0 . The resulting MEP is obtained by following the gradient by steepest descent.

-
- ¹ M. Respaud, J. M. Broto, H. Rakoto, A. R. Fert, L. Thomas, B. Barbara, M. Verelst, E. Snoeck, P. Lecante, A. Mosset, J. Osuna, T. O. Ely, C. Amiens, and B. Chaudret, Phys. Rev. B **57**, 2925 (1998); T. Aign, P. Meyer, S. Lemerle, J. P. Jamet, J. Ferré, V. Mathet, C. Chappert, J. Gierak, C. Vieu, F. Rousseaux, H. Launois, and H. Bernas, Phys. Rev. Lett. **81**, 5656 (1998); M. Giersig and M. Hilgersdorff, J. Phys. A **32**, L111 (1999); S. Padovani, I. Chado, F. Scheurer, and J. P. Bucher, Phys. Rev. B **59**, 11887 (1999); V. Russier, C. Petit, J. Legrand, and M. P. Pileni, Phys. Rev. B **62**, 3910 (2000); S. Sun, C. B. Murray, D. Weller, L. Folks, and A. Moser, Science **287**, 1989 (2000); D. Babonneau, J. Briatico, F. Petroff, T. Cabioch, and A. Naudon, J. Appl. Phys. **87**, 3432 (2000); V. F. Puentes, K. M. Krishnan, and A. P. Alivisatos, Science **291**, 2115 (2001); F. Luis, J. M. Torres, L. M. García, J. Bartolomé, J. Stankiewicz, F. Petroff, F. Fetta, J. L. Maurice, and A. Vaurès, Phys. Rev. B **65**, 094409 (2002); P. Gambardella, A. Dallmeyer, K. Maiti, M. C. Malagoli, W. Eberhardt, K. Kern, and C. Carbone, Nature **416**, 301 (2002).

- ² J. L. Dorman, D. Fiorani, and E. Tronc, Adv. Chem. Phys. **98**, 283 (1997); J. Magn. Magn. Mater. **202**, 251 (1999); M. F. Hansen and S. Mørup, J. Magn. Magn. Mater. **184**, 262 (1998).
- ³ D. K. Lottis, R. M. White, and E. D. Dahlberg, Phys. Rev. Lett. **67**, 362 (1991).
- ⁴ T. Jonsson, J. Mattsson, C. Djurberg, F. A. Khan, P. Nordblad, and P. Svedlindh, Phys. Rev. Lett. **75**, 4138 (1995); C. Djurberg, P. Svedlindh, P. Nordblad, M. F. Hansen, F. Bødker, and S. Mørup, Phys. Rev. Lett. **79**, 5154 (1997); P. E. Jönsson, H. Yoshino, H. Mamiya, and H. Takayama, Phys. Rev. B. **71**, 104404 (2005); M. Sasaki, P. E. Jönsson, H. Takayama, and H. Mamiya, Phys. Rev. B. **71**, 104405 (2005).
- ⁵ K. Binder and A. P. Young, Rev. Mod. Phys. **58**, 801 (1986); A. P. Young, *Spin Glasses and Random Fields* (World Scientific, Singapore, 1997).
- ⁶ Weili Luo, S. R. Nagel, T. F. Rosenbaum, and R. E. Rosensweig, Phys. Rev. Lett. **67**, 2721 (1991); Jinlong Zhang, C. Boyd, and Weili Luo, Phys. Rev. Lett. **77**, 390 (1996); B. Martinez, X. Obradors, L. Balcells, A. Rouanet, and C. Monty, Phys. Rev. Lett. **80**, 181 (1998); H. Mamiya, I. Nakatani, and T. Furubayashi, **82**, 4332 (1999); M. García del Muro, X. Batlle, and A. Labarta, Phys. Rev. B **59**, 13 584 (1999); P. Jönsson, M. F. Hansen, and P. Nordblad, Phys. Rev. B **61**, 1261 (2000); P. Allia, M. Coisson, P. Tiberto, F. Vinai, M. Knobel, M. A. Novak, and W. C. Nunes, Phys. Rev. B **64**, 144420 (2001);
- ⁷ W. Kleemann, O. Petravic, Ch. Binek, G. N. Kakazei, Yu. G. Pogorelov, J. B. Sousa, S. Cardoso, and P. P. Freitas, Phys. Rev. B **63**, 134423 (2001); F. Luis, F. Petroff, J. M. Torres, L. M. García, J. Bartolomé, J. Carrey, and A. Vaurés, Phys. Rev. Lett. **88**, 217205 (2002); P. Poddar, T. Telem-Shafir, T. Fried, and G. Markovich, Phys. Rev. B **66**, 060403(R) (2002).
- ⁸ C. Binns, M. J. Maher, Q. A. Pankhurst, D. Kechrakos, and K. N. Trohidou, Phys. Rev. B **66**, 184413 (2002).
- ⁹ J. A. C. Bland and B. Heinrich, *Ultrathin Magnetic Structures I + II* (Springer, Berlin, 1994).
- ¹⁰ S. Rusponi, T. Cren, N. Weiss, M. Epple, P. Bulushek, L. Claude, H. Brune, Nature Materials **2** (2003).
- ¹¹ O. Pietzsch, S. Okatov, A. Kubetzka, M. Bode, S. Heinze, A. Lichtenstein, and R. Wiesen-

- danger, Phys. Rev. Lett. **96**, 237203 (2006).
- ¹² J. Bansmann, S.H. Baker, C. Binns, J. A. Blackman, J.-P. Bucher, J. Dorantes-Dávila, V. Dupuis, L. Favre, D. Kechrakos, A. Kleibert, K.-H. Meiwes-Broer, G.M. Pastor, A. Perez, O. Toulemonde, K. N. Trohidou, J. Tuailon and Y. Xie, Surf. Sci. Rep. **56** 189 (2005) 189.
 - ¹³ P. Bruno, Phys. Rev. B **52**, 411 (1995).
 - ¹⁴ V. I. Safonov and H. N. Bertram, J. Appl. Phys. **87**, 5508 (2000); X. Waintal and P. W. Brouwer, Phys. Rev. Lett. **91**, 247201 (2003); A. Cehovin, C. M. Canali, and A. H. MacDonald, Phys. Rev. B **69**, 045411 (2004).
 - ¹⁵ J. O. Andersson, C. Djurberg, T. Jonsson, P. Svedlindh, and P. Nordblad, Phys. Rev. B **56**, 13983 (1997); J. García-Otero, M. Porto, J. Rivas, and A. Bunde, Phys. Rev. Lett. **84**, 167 (2000); D. Kechrakos and K. N. Trohidou, Phys. Rev. B **62**, 3941 (2000); S. I. Denisov, T. V. Lyutyy, and K. N. Trohidou, Phys. Rev. B **67**, 014411 (2003); M. Ulrich, J. García-Otero, J. Rivas, and A. Bunde, Phys. Rev. B **67**, 024416 (2003); O. Iglesias and A. Labarta, Phys. Rev. B **70**, 144401 (2004).
 - ¹⁶ P. J. Jensen and G. M. Pastor, Phys. Stat. Sol. (a) **189**, 527 (2002); New J. Phys. **5**, 68 (2003).
 - ¹⁷ D. Kechrakos and K. N. Trohidou, Phys. Rev. B **58**, 12169 (1998); V. Russier, J. Appl. Phys. **89**, 1287 (2001); V. Russier, C. Petit, and M. P. Pileni, J. Appl. Phys. **93**, 10001 (2003); A. A. Fraerman and M. V. Sapozhnikov, Phys. Rev. B **65**, 184433 (2002).
 - ¹⁸ M. A. Załuska-Kotur, Phys. Rev. B **54**, 1064(1996); R. Prozorov, Y. Yeshurun, T. Prozorov, and A. Gedanken, Phys. Rev. B **59**, 6956 (1999); S. I. Denisov and K. N. Trohidou, Phys. Rev. B **64**, 184433 (2001); L. Wang, J. Ding, H. Z. Kong, Y. Li, and Y. P. Feng, Phys. Rev. B **64**, 214410 (2001).
 - ¹⁹ R. W. Chantrell, N. Walmsley, J. Gore, and M. Maylin, Phys. Rev. B **63**, 024410 (2000).
 - ²⁰ J. L. Dorman, L. Bessais, and D. Fiorani, J. Phys. C **21**, 2015 (1988); J. O. Andersson, C. Djurberg, T. Jonsson, P. Svedlindh, and P. Nordblad, Phys. Rev. B **56**, 13983 (1997); A.O. Ivanov and O. B. Kuznetsova, Phys. Rev. E **64**, 041405 (2001).
 - ²¹ D. V. Berkov, J. Magn. Magn. Mater. **186**, 199 (1998); R. Dittrich, T. Schrefl, D. Suess, W. Scholz, H. Forster, and J. Fidler, J. Magn. Magn. Mater. **250**, 12 (2002).

- ²² E. C. Stoner and E. P. Wohlfarth, Trans. Roy. Soc. A **240**, 599 (1948).
- ²³ P. J. Jensen, Ann. Physik (Leipzig) **6**, 317 (1997).
- ²⁴ P. J. Jensen and G.M. Pastor, Phys. Rev. B **68**, 184420 (2003).
- ²⁵ C. J. Cerjan and W. H. Miller, J. Chem. Phys. **75**, 2800 (2000); J. P. K. Doye and D. J. Wales, Z. Phys. B **40**, 194 (1997); N. Mousseau and G. T. Barkema, Phys. Rev. E **57**, 2419 (1998).
- ²⁶ D. J. Wales, in *Atomic Clusters and Nanoparticles*, edited by C. Guet, P. Hobza, F. Spiegelman, and F. David, (Springer, Berlin, 2000), p. 438; *Energy Landscapes* (Cambridge University Press, Cambridge, 2003).